Fuel 313 (2022) 122708

Contents lists available at ScienceDirect

Fuel

journal homepage: www.elsevier.com/locate/fuel

Full Length Article

Numerical simulation of bitumen recovery via supercritical water injection with in-situ upgrading

Haoming Ma [a], Yun Yang [b,*], Zhangxin Chen [a,*]

[a] Department of Chemical and Petroleum Engineering, University of Calgary, 2500 University Drive NW, Calgary, Alberta T2N 1N4, Canada
[b] Department of Geoscience, University of Calgary, 2500 University Drive NW, Calgary, Alberta T2N 1N4, Canada

ARTICLE INFO

Keywords:
Supercritical water flooding
Aquathermolysis
In-situ upgrading
Miscible flooding
Sensitivity analysis

ABSTRACT

As the demand of crude oil is increasing along with depletion of conventional oil, unconventional oil is being extracted to meet the demand worldwide. Heavy oil is one of the largest unconventional crude oil resources, especially in Canada and Venezuela. Thermal recovery is a promising technology developed over the past decades. Particularly, steam injection is considered one of the most effective thermal recovery processes, but it is energy-intensive and is not environmentally friendly. Unlike steam injection, supercritical water flooding (SCWF) is a miscible flooding and in-situ upgrading process and has been experimentally proven as a more effective process than steam injection. However, it has not been field-proven yet. Therefore, numerical simulation is necessary to show its feasibility. In this paper, we present a numerical simulation workflow for SCWF by utilizing CMG-STARS and study its sensitive parameters based on simulation outputs. Simulation results show that SCWF has a better performance due to its gas production from aquathermolysis. Its recovery efficiency can double when compared to steam injection owing to its in-situ upgrading feature within the same production window. SCWF is more suitable in thinner, lower porosity and higher permeability reservoirs. Operational parameters are slightly influencing its reservoir performance, and the influence is negligible as long as a minimum miscible pressure (MMP) is achieved.

1. Introduction

The latest reports by International Energy Agency (IEA) and U.S. Energy Information Administration (EIA) predicted that the global energy demand is surpassing the pre-COVID-19 level with the recovery of the global economy and the oil demand is rebounding faster than all other fuels [1,2]. Unconventional oil resources, such as heavy oil and bitumen, account for 70% of recoverable petroleum resources and are attracting global interest as one of the best alternatives to conventional oil [3]. According to the World Energy Outlook (2020), the current crude oil resources are estimated at over six trillion barrels worldwide, and over 1.8 trillion barrels are extra-heavy oil and bitumen, which is about 30% of the total crude oil resources [4]. Over 1.2 trillion barrels are found in America. Canada and Venezuela are the two largest heavy oil producers, and almost 50% of the daily crude oil production (total crude oil production: over five million barrels per day) was from heavy oil, and bitumen in Canada in 2019. According to IEA, the predictions from both stated policies and sustainable development scenarios suggested that heavy oil and bitumen will account for four million barrels per day in the world oil production in 2040, which is a 60% increase compared to the 2010 level [4,5]. The U.S. Geological Survey (USGS) defined heavy oil as crude oil with its API gravity between 10 and 20 API and viscosity over 100 cP; bitumen has an API of less than 10 API but viscosity greater than 10,000 cP [6]. Majority of heavy oil and bitumen are located in Alberta and Saskatchewan in Canada and the northern bank of Orinoco River in Venezuela. Owing to their high viscosity and density, heavy oil and bitumen are hard to flow in reservoir conditions due to their ultralow mobility [7,8].

Effective heavy oil recovery always requires a significant reduction in viscosity and a significant improvement in mobility. Its viscosity can be significantly reduced when reservoir temperature increases. Thus, thermal recovery is commonly adopted in an enhanced oil recovery

Abbreviations: IEA, International Energy Agency; EIA, U.S. Energy Information Administration; USGS, U.S. Geological Survey; EOR, Enhanced Oil Recovery; CHOPS, Cold Heavy Oil Production with Sands; ISC, In-Situ Combustion; CSS, Cyclic Steam Stimulation; SAGD, Steam Assisted Gravity Drainage; SCWF, Supercritical Water Flooding; RF, Recovery Factor; OOIP, Original Oil In Place; MMP, Minimum Miscible Pressure; SOR, Steam-Oil Ratio.

* Corresponding authors.
E-mail addresses: yun.yang@ucalgary.ca (Y. Yang), zhachen@ucalgary.ca (Z. Chen).

https://doi.org/10.1016/j.fuel.2021.122708
Received 27 September 2021; Received in revised form 7 November 2021; Accepted 22 November 2021
Available online 1 December 2021

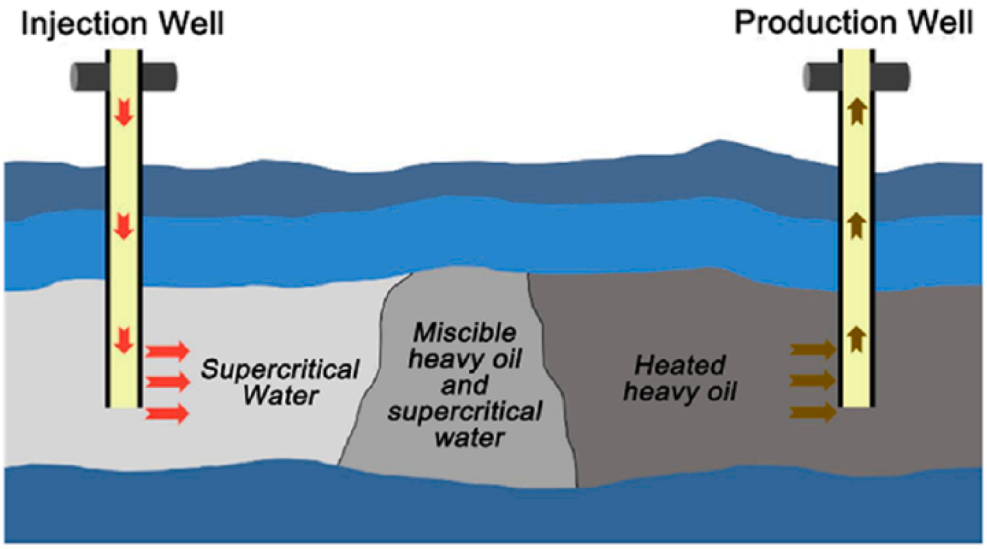

Fig. 1. Mechanisms of SCWF (credit to Zhao et al.[15]).

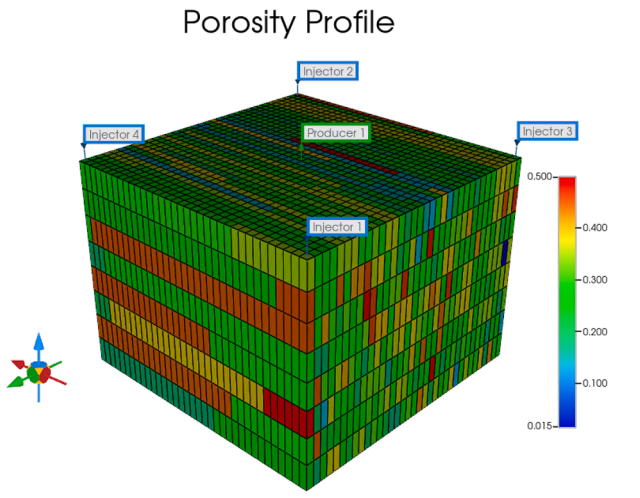

Fig. 2. Heterogeneous 3D reservoir model and well locations.

Table 1
Reservoir properties.

Parameters	Value
Reservoir Area – A [m^2]	19,600
Reservoir Depth – D [m]	500
Reservoir Thickness – H [m]	30
Reservoir Temperature – T [°C]	37
Initial Pressure - P_{ini} [kPa]	8,576
Average Porosity – φ [%]	30
Average Horizontal Permeability - k_h [%]	400
Average Vertical Permeability - k_v [%]	40
Molar mass of Bitumen – M [kg/kmole]	533
Density of Bitumen - ρ [kg/m^3]	1,026
Rock Compressibility [kPa^{-1}]	1.80×10^{-5}
Rock Heat Capacity [J/(m^3 °C)]	2.35×10^6
Underburden Heat Capacity [J/(m^3 °C)]	2.35×10^6
Overburden Heat Capacity [J/(m^3 °C)]	2.35×10^6
Thermal Conductivity of Matrix [J/(day °C)]	6.60×10^4
Thermal Conductivity of Water [J/(day °C)]	5.35×10^4
Thermal Conductivity of Water [J/(day °C)]	8.04×10^3
Gridding Size - I, J, K [m]	$4 \times 4 \times 3.75$
Simulation Window [years]	3

(EOR) process aimed to increase the reservoir temperature by injecting high temperature fluids. The first cyclic steam injection pilot project was operated by Trintopec in the Palo Seco field in 1966 [9]. Pioneered works proved that a number of processes can be applied at the field level to improve heavy oil recovery efficiency, such as cold heavy oil production with sands (CHOPS), in-situ combustion (ISC), chemical injection and flooding, and gas injection [10–14]. The traditional heavy oil EOR processes can be classified to three groups based on their mechanisms: thermal recovery processes are to reduce the oil viscosity, miscible flooding processes improve the EOR performance by eliminating interfacial tension, and chemical injection processes decrease the interfacial tension [15]. Over the past decades thermal processes are widely selected in field applications. Cyclic steam stimulation (CSS), steam assisted gravity drainage (SAGD) and steam flooding are three proven field thermal EOR processes since the 1960s [7,16–18]. In-situ upgrading which first proposed in 1982 by Hyne et al. is another process that allows both upgrading and recovery simultaneously, their work demonstrated that a steam reaction also triggered a chemical reaction with oil [19]. Researchers introduced expensive catalysts to improve the recovery efficiency since the possibility of in-situ upgrading could be achieved [13]. For example, Elahi et al. introduced a kinetic model of the in-situ upgrading process of nano-catalysts and experimentally proved that the viscosity of heavy oil is significantly reduced and the API gravity increased [20]. Previous studies also proved that supercritical water can be utilized as a high temperature solvent for heavy oil recovery, so that both heavy oil upgrading and viscosity reduction are achieved at the same time with lower cost comparing to employing expensive catalysts [21–23].

Supercritical water flooding (SCWF) is a miscible flooding process reducing the heavy oil viscosity and upgrading it without severe carbon loss during EOR operations. Supercritical water defines water above its critical point (374 °C and 22.1 MPa). With this condition, a gas–liquid phase interface no longer exist, and hydrogen bonds break down. Supercritical water more easily flows in porous media and transports heat and mass than hot water and steam because of no surface intension and higher density. The mechanisms of SCWF include both reducing oil viscosity by a thermal process and decreasing seepage resistance (Fig. 1). Compared to traditional thermal recovery processes, supercritical water is considered as both a heat carrier and a hydrogen donor for the EOR. It also creates an ideal homogeneous exploiting and thermal cracking environment for heavy oil at reservoir conditions. In addition, carbon loss due to coking caused low recovery efficiency and high energy consumption in a traditional thermal process. SCWF can effectively

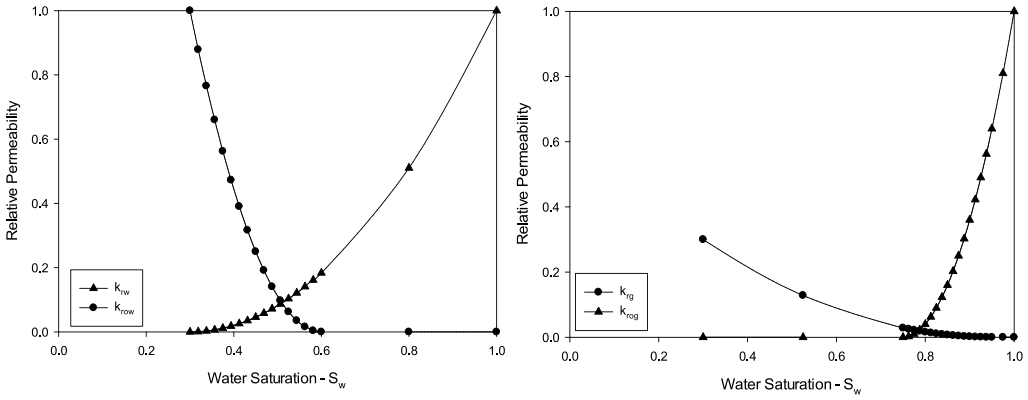

Fig. 3. Relative permeabilities of (1) water and oil (left) and (2) liquid and gas (right).

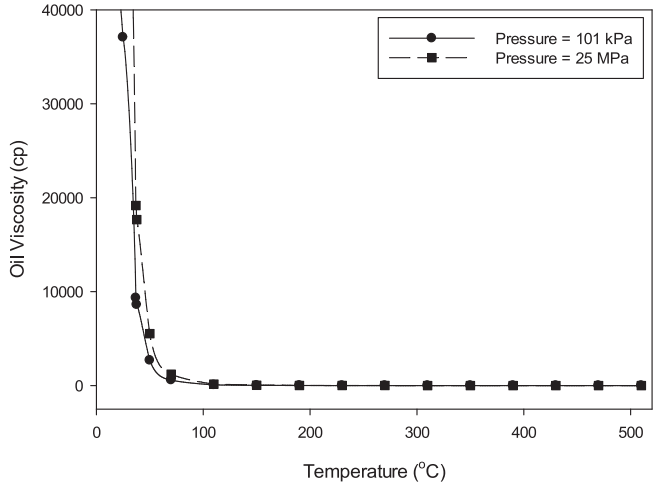

Fig. 4. Viscosity of Cold Lake bitumen vs. temperature.

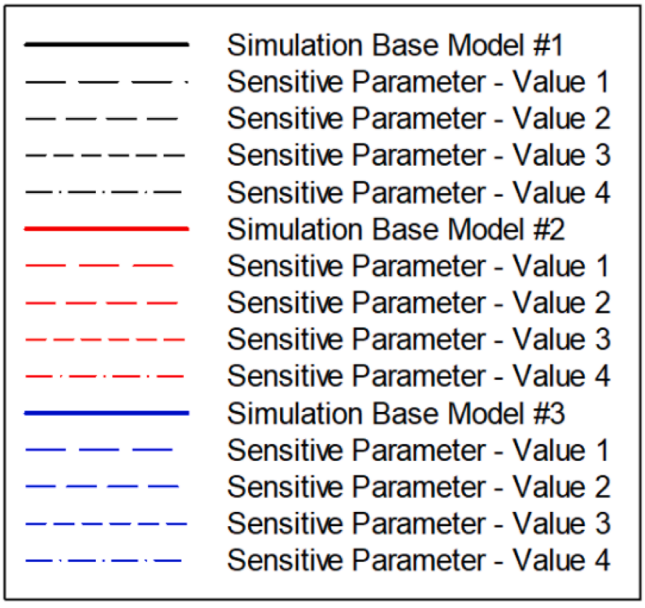

Fig. 5. Legend of the result plots.

Table 2
Values of sensitive parameters.

Sensitive Parameter	Reference Value	Value 1	Value 2	Value 3	Value 4
Thickness – H [m]	30	10	20	40	50
Average Porosity - φ	0.3	0.1	0.2	0.4	0.5
Average Horizontal Permeability - k_h [mD]	400	200	300	500	600
Initial Pressure – P_{ini} [kPa]	8,576	7,500	8,000	9,000	9,500
Injection Rate – R_{inj} [m3/day]	100	60	140	–	–
Injection Pressure – P_{inj} [MPa]	25	30	35	–	–
Steam Temperature – T_{inj} [C]	420	385	480	–	–

avoid carbon loss in its recovery process [15,24–31]. Zhao et al. demonstrated that SWCF can potentially improve the oil recovery by 17% while reducing the thermal energy consumption by 34% through core flooding experiments. However, there is no evidence yet showing that SCWF is applicable to the field. Therefore, numerical simulation has become the sole tool to study its feasibility thus far.

In this work, we proposed a field level 5-spot numerical simulation workflow with utilizing the CMG-STARS simulator to address the potential influential factors of the SCWF application in bitumen recovery. We performed a sensitivity analysis based on the reservoir performance (i.e., cumulative bitumen recovery and a cumulative steam-oil ratio) while considering geological properties (i.e., thickness, porosity, permeability, and initial reservoir pressure) and operational parameters (i.e., an injection rate, injection pressure and injection temperature). Total three scenarios and 63 simulation runs were carried out, and the sensitive parameters were determined based on simulation results.

2. Methodologies and numerical simulation

2.1. Governing equations

There are three types of governing equations involved in the basic numerical simulation: the mass conservation for water, steam and oil; the energy conservation; and Darcy's equation. The water and steam equilibrium can be determined according to steam table data [32,33].

$$\text{Mass conservation}: \frac{\partial}{\partial t}(\phi\rho_i S_i) - \nabla(\rho U_i) - \rho_i q_i = 0 \quad (1)$$

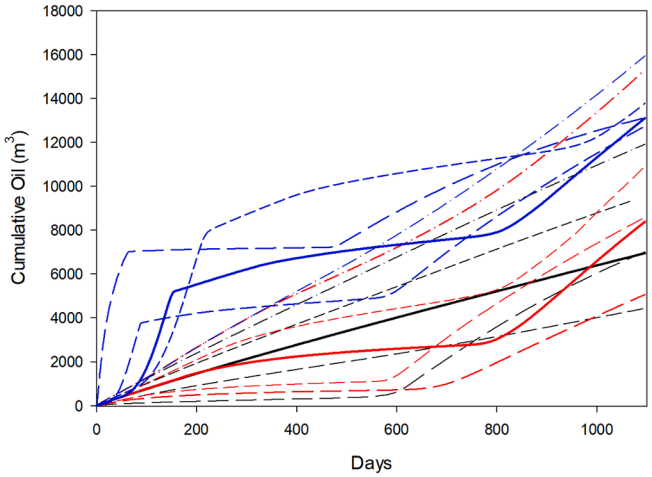

(a) Cumulative oil production under different thicknesses

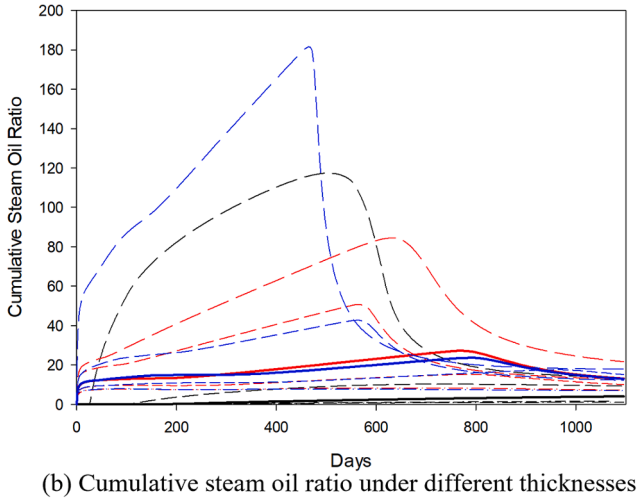

(b) Cumulative steam oil ratio under different thicknesses

Fig. 6. Sensitivity analysis of thickness.

$$\text{Water phase}: \frac{\partial}{\partial x}(A_x k_x \frac{k_{rw}\rho_w}{\mu_w}\frac{\partial p}{\partial x})\Delta x + \frac{\partial}{\partial y}(A_y k_y \frac{k_{rw}\rho_w}{\mu_w}\frac{\partial p}{\partial y})\Delta y + \frac{\partial}{\partial z}(A_z k_z \frac{k_{rw}\rho_w}{\mu_w}(\frac{\partial p}{\partial z} - \gamma_w \frac{\partial h}{\partial z}))\Delta z = V_b \frac{\partial}{\partial t}(\phi\rho_w S_w - \rho_w q_{conv}) \quad (5)$$

$$\text{Steam phase}: \frac{\partial}{\partial x}(A_x k_x \frac{k_{rs}\rho_s}{\mu_s}\frac{\partial p}{\partial x})\Delta x + \frac{\partial}{\partial y}(A_y k_y \frac{k_{rs}\rho_s}{\mu_s}\frac{\partial p}{\partial y})\Delta y + \frac{\partial}{\partial z}(A_z k_z \frac{k_{rs}\rho_s}{\mu_s}(\frac{\partial p}{\partial z} - \gamma_s \frac{\partial h}{\partial z}))\Delta z = V_b \frac{\partial}{\partial t}(\phi\rho_s S_s - \rho_s q_{conv}) \quad (6)$$

2.2. Model description

The thermal simulator, CMG-STARS, is used in this research to investigate the performance of bitumen recovery with SWCF. The gridding system of the base reservoir model was 35 × 35 × 8. The 3D heterogeneous reservoir was developed consisting only of reservoir sands with a 5-spot well pattern (four injectors from layers 4 to 8 and one producer from layers 4 to 6, Fig. 2). The base data source was refined from a CMG course "Introduction to Thermal EOR Modeling" with the oil component and its viscosity adopted from Cold Lake Bitumen [34,35]. The Cold Lake bitumen is one of the most typical bitumen samples in Canada and has been widely used for research purposes. The experimental data, especially the viscosity data of the Cold Lake bitumen properties, is well-established, and the results are proven with high accuracy [14,35–38]. Table 1 describes the detailed reservoir properties. Fig. 3 shows the relative permeability curves that we adopted in the simulation. The following three scenarios were compared: (1) steam flooding with 0.8 steam quality, 300 °C steam temperature and an injection bottomhole pressure of 12 MPa; (2) supercritical water injection without considering aquathermolysis in-situ upgrading; and (3) supercritical water injection with considering aquathermolysis in-situ upgrading. The injection pressure for scenarios 2 and 3 was equivalent at 25 MPa, which is above the bubble point pressure (22.1 MPa) of water, and the steam temperature was 430 °C, which is also above the bubble point temperature (374 °C). Water exists in the supercritical phase above its bubble point; thus, the steam quality is equal to 1 for the SCWF scenarios. The injection rate for all scenarios is defined as 100 m^3/day. The reservoir performance was evaluated based on cumulative oil production and the cumulative steam-oil ratio for each scenario. Two groups of variables were studied in our investigation. The geological properties include thickness – H, porosity – φ, permeability – k, and initial reservoir pressure - P_{ini}. The operational parameters include the maximum injection rate – R_{inj}, injection steam pressure – P, and steam temperature – T.

$$\text{Energy conservation}: \nabla K_h \nabla T - \nabla \sum_i (\rho_i u_i h_i) + Q = \frac{\partial}{\partial t}[\phi(\sum_i \rho_i S_i U_i) + (1-\phi)\rho_R U_R] \quad (2)$$

$$\text{Darcy equation}: u_i = -\frac{k k_{ri}}{\mu_i}[\nabla p_i - \rho_i g \nabla Z_i] \quad (3)$$

In Eq. (1), three terms are defined as accumulation, input/output, and production/injection, respectively. The fluid velocity in Eqs. (1) and (2) is given by Darcy's equation. Thus, the mass equations for three phases in three dimensions (3D) are given below:

$$\text{Oil phase}: \frac{\partial}{\partial x}(A_x k_x \frac{k_{ro}\rho_o}{\mu_o}\frac{\partial p}{\partial x})\Delta x + \frac{\partial}{\partial y}(A_y k_y \frac{k_{ro}\rho_o}{\mu_o}\frac{\partial p}{\partial y})\Delta y + \frac{\partial}{\partial z}(A_z k_z \frac{k_{ro}\rho_o}{\mu_o}(\frac{\partial p}{\partial z} - \gamma_o \frac{\partial h}{\partial z}))\Delta z = V_b \frac{\partial}{\partial t}(\phi\rho_o S_o - \rho_o q_o) \quad (4)$$

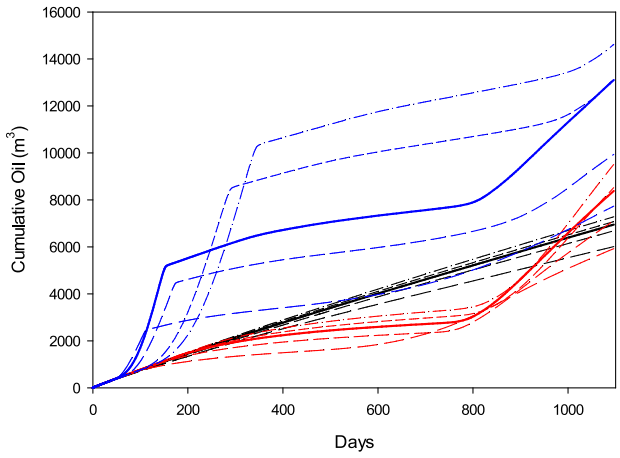

(a) Cumulative oil production under different porosities

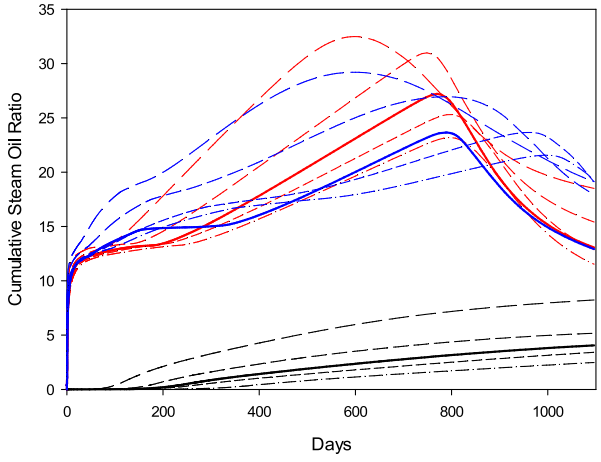

(b) Cumulative steam-oil ratios under different porosities

Fig. 7. Sensitivity analysis of porosity.

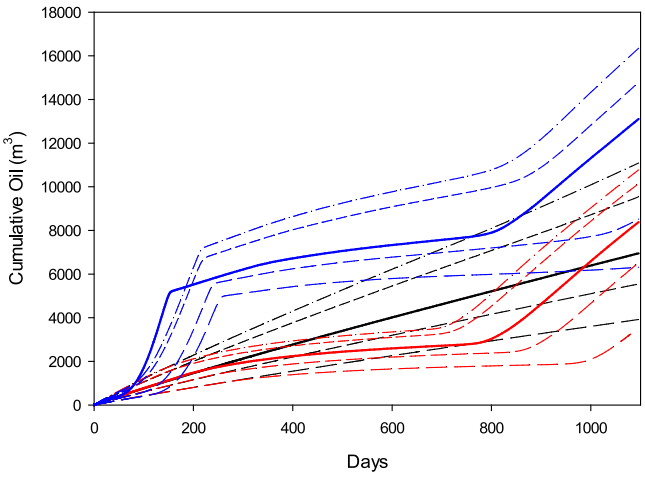

(a) Cumulative oil production under different permeabilities

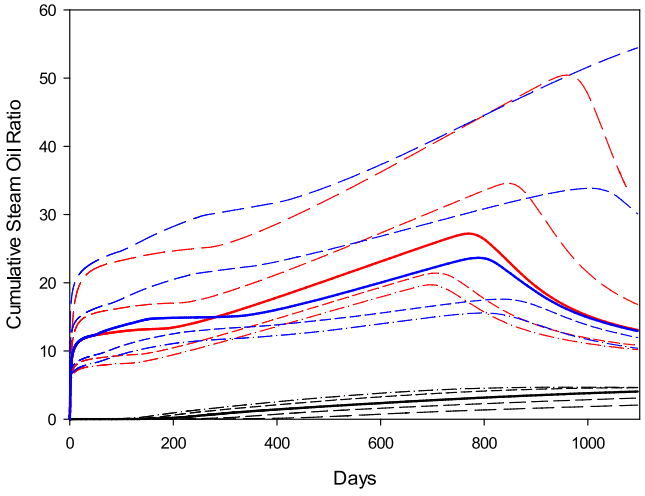

(b) Cumulative steam-oil ratios under different permeabilities

Fig. 8. Sensitivity analysis of permeability.

2.3. Properties of the Cold Lake bitumen

The oil component involved in the reservoir model is from the Cold Lake region in Alberta, Canada. The Cold Lake bitumen has been studied since the 1970s, and the properties of a bitumen sample has been studied and well established according to the literature [34–38]. Its average molar mass is 533 kg/kmol, and its density is linearly calibrated approximately to 1026 kg/m^3 at the standard condition. The boiling point is below 600 °C. The bitumen viscosity dramatically declines with the increasing temperature and decreasing pressure. The relationship of viscosity, temperature and pressure of the Cold Lake bitumen was derived by Mehrotra and Svrcek as follows [35]:

$$ln(\mu) = exp[22.64 - 3.56lnT] + 0.029P \quad (7)$$

where μ is the bitumen viscosity, cp; T is temperature, °C; and P is pressure, MPa. The correlation of the bitumen viscosity and temperature is thus described in Fig. 4 at atmospheric pressure and 25 MPa. The viscosity of the Cold Lake bitumen was calculated based on equation (7) with changing temperature from 25 °C to 500 °C. According to Fig. 4, a higher viscosity is observed at higher pressure with the isothermal condition. The results are consistent with the experimental observations published by Mehrotra et al. [35], and the viscosity significantly decreased from 3700cp to 20cp and was approximate to 0 cp starting from 180 °C under the standard condition pressure. When the fluid temperature exceeds 150 °C, the increasing pressure will no longer trigger the significant impact on the bitumen viscosity.

2.4. Aquathermolysis

We considered the aquathermolysis chemical reaction in scenario 3 due to the in-situ upgrading process. The chemical reaction is believed to occur when the reservoir temperature exceeds 300 °C [39,40]. The mechanisms of heavy oil upgrading by supplying supercritical water can be attributed to two aspects, effects of physical properties and chemical effects. The chemical role of supercritical water as a hydrogen donor has been proven when the temperature exceeds 425 °C [24,41]. Gas components including methane, carbon dioxide, hydrogen sulfide, hydrogen and a small amount of low molecular weight hydrocarbons will be

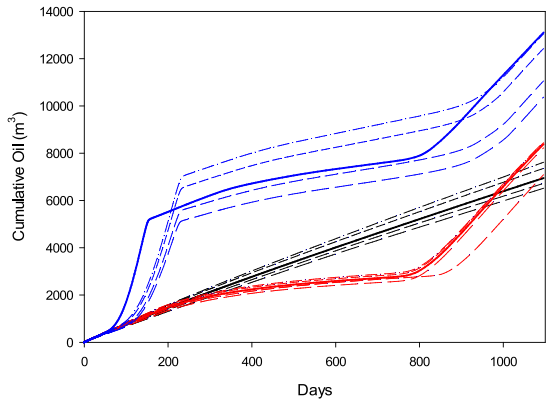

(a) Cumulative oil production under different initial reservoir pressures

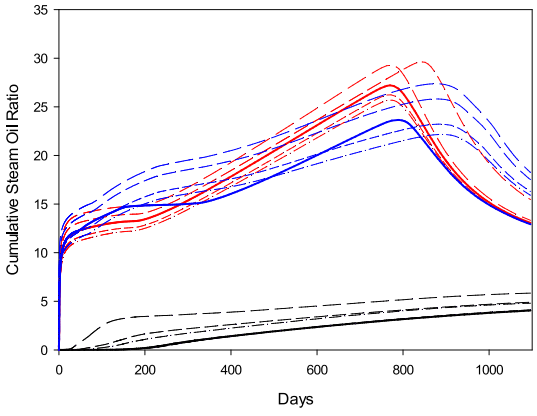

(b) Cumulative steam-oil ratios under different initial reservoir pressures

Fig. 9. Sensitivity analysis of initial reservoir pressure.

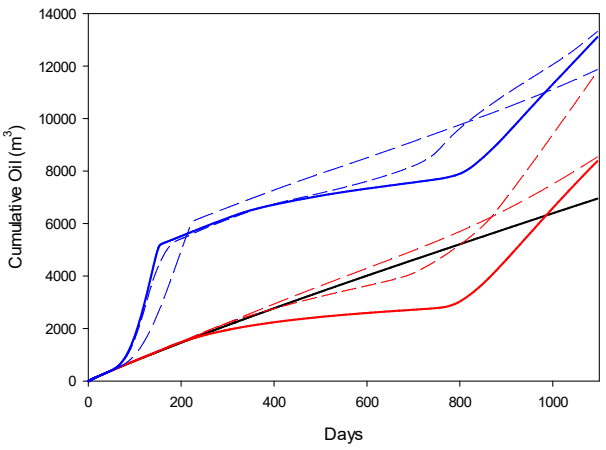

(a) Cumulative oil production under different injection rates

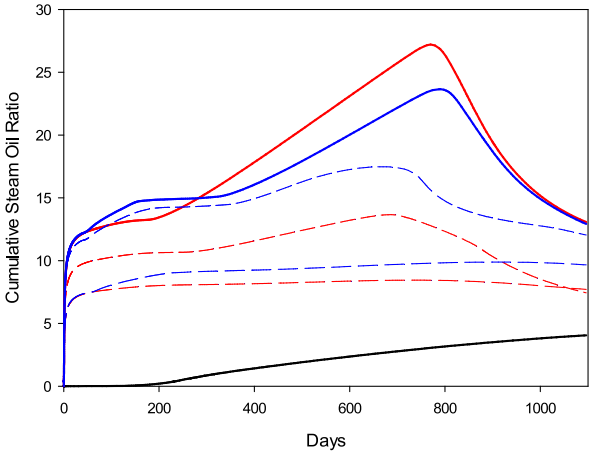

(b) Cumulative steam-oil ratios under different injection rates

Fig. 10. Sensitivity analysis of injection rate.

produced from the aquathermolysis reaction. We defined the reaction in CMG-STARS with the bitumen and supercritical water as the reactants and the gas mixture as the final product.

$$RCH_2CH_2SCH_3 + 2H^+ + 2OH^- \leftrightarrow RCH_3 + CO_2 + H_2 + CH_4 + H_2S \quad (8)$$

The results of scenario 3 reported from CMG-STARS provided a gas volume production rate with the unit of m^3. We calculated the equivalent volumetric oil due to the aquathermolysis reaction at the standard conditions according to the ideal gas law.

$$n_{gas} = \frac{RT_{sc}}{V_{gas,sc}P_{sc}} \quad (9)$$

$$V_{oil,sc} = n_{oil} \times \frac{M_{oil}}{\rho_{oil}} \quad (10)$$

where n is the number of moles; M is the molar mass; V_{sc} is the volume at the standard conditions; ρ_{sc} is the bitumen density at the standard conditions; T_{sc} is the standard condition temperature equal to 288 K; P_{sc} is the standard condition pressure equal to 1 atm; and R is the gas constant equal to 8.21×10^{-5} [(m^3•atm)/(mole•K)]. We adopted the molar balance of the reactions and calculated all the chemical products from the gas phase. Implementing these into CMG-STARS, we need the molar mass of the reactants and the products. Since we consider all the gas products as one product, we only simulate one chemical reaction in CMG.

3. Result and discussion

Totally, seven sensitive parameters were studied in each scenario with their values in Table 2. A total of 63 simulation runs were performed in this study, and the detailed results are provided in Table A.1. The cumulative oil production and steam-oil ratio were employed as the output results from the simulation, the recovery factor (RF) was calculated accordingly for each run, and the sensitivity analysis of RF was conducted based on these output results within the three-year production window. The recovery factor is defined as the ratio of cumulative oil production to the original oil in place (OOIP) within the simulation time window. The legend of result plots was presented in Fig. 5. Scenarios 1, 2 and 3 are presented by the color of black, red, and blue, respectively. In

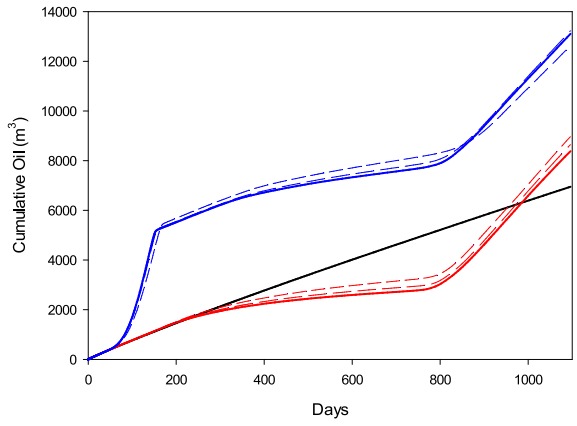

(a) Cumulative oil production under different injection pressures

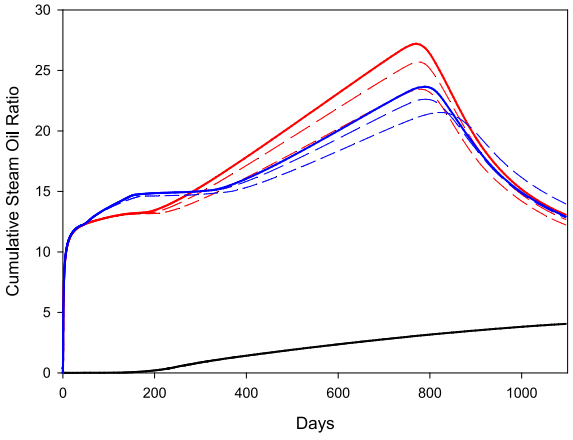

(b) Cumulative steam-oil ratios under different injection pressures

Fig. 11. Sensitivity analysis of injection pressure.

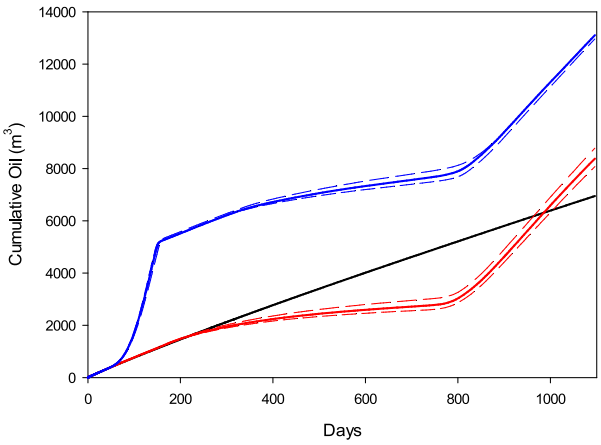

(a) Cumulative oil production under different steam pressures

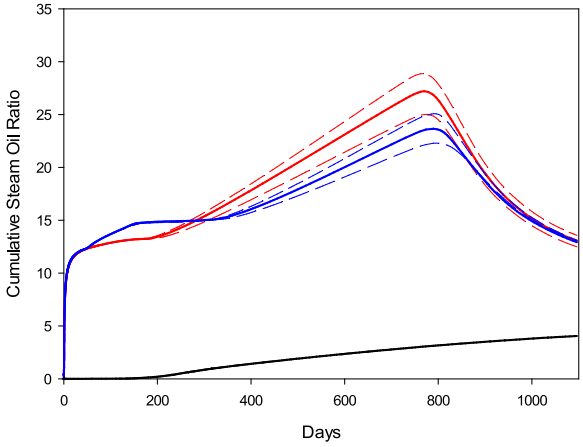

(b) Cumulative steam-oil ratios under different steam pressures

Fig. 12. Sensitivity analysis of steam pressure.

this part, the cumulative oil production and steam-oil ratio curves were plotted during the three-year production window. We highlighted the reference simulation result in each scenario and analyzed the sensitivity of multiple parameters based on simulation observation. The mechanism of steam flooding is immiscible flooding, whereas the supercritical water injection triggered the miscible flooding since the injection steam pressure is over the minimum miscible pressure (MMP) [15]. The MMP of water and the Cold Lake bitumen was calculated by CMG-Winprop simulator, which is about 18 MPa at 350 °C. We observed that the injected supercritical water steam will not perform as well as steam flooding as an EOR process in the early period due to its miscibility with bitumen. After the steam breakthrough point (i.e., in our case, about 800 days after steam injection), there will be a significantly incremental recovery due to the greater mobility of the bitumen and water mixture. The overall performance of applying supercritical water will be better in a long-term production window. With considering the aquathermolysis, the injected supercritical water can react with bitumen and produce gas. Thus, the cumulative oil production will be higher than steam flooding in the early stage. However, in scenario 3, the gas phase products from aquathermolysis are depleted within about 150 days, and hence its cumulative oil production shares a similar shape to scenario 2. The cumulative steam-oil ratios (SOR) held a similar shape for both scenarios 2 and 3 and demonstrated that in the early days the injected supercritical water is miscible with the bitumen. For the immiscible process (i.e., scenario 1), a lower cumulative SOR was observed all the time due to its immediate contribution to the bitumen recovery. Overall, the cumulative SOR of utilizing supercritical water is always higher than traditional steam flooding due to the miscible process.

$$RF = \frac{\sum_{t=1}^{t=3} P_{oil,t}}{OOIP} \tag{11}$$

3.1. Geological property – thickness

In this part, the impact of reservoir thickness was examined. We studied the reservoirs with thickness varying from 10 m to 50 m for all three scenarios. As a result, the total recovered bitumen is not fluctuated significantly within each scenario. However, the OOIP is negatively correlated with thickness, which will lead to a lower recovery factor in

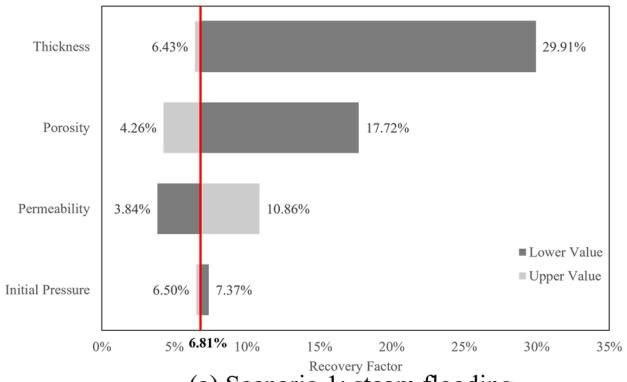

(a) Scenario 1: steam flooding

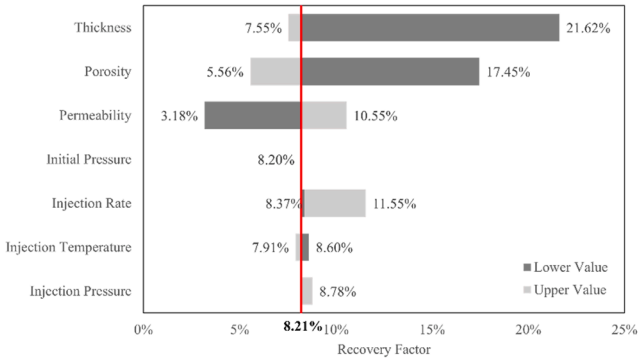

(b) Scenario 2: SCWF without aquathermolysis

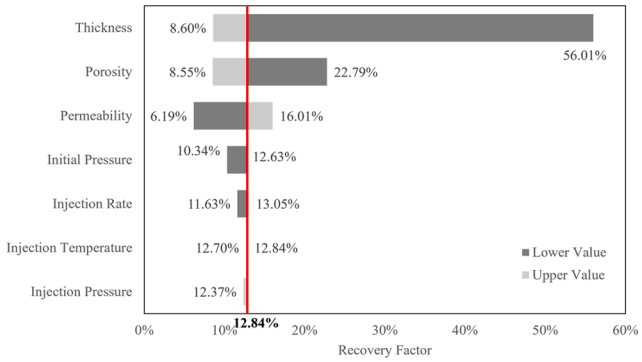

(c) Scenario 3: SCWF with aquathermolysis

Fig. 13. Tornado diagrams.

thicker reservoirs. In addition, the miscibility of bitumen and supercritical water is not efficient for large thickness reservoirs. From Fig. 6 (b), the cumulative SOR in a low thickness reservoir is large owing to the early water breakthrough. Compared to other scenarios, scenario 3 requires more supercritical water in the early production stage due to the aquathermolysis chemical reaction.

Overall, the result proved that the cumulative oil produced under different thicknesses will not vary a lot in the three-year production period. It is reasonable to extract more oil from thicker reservoirs for all scenarios; however, a higher recovery factor is desired for thinner reservoirs due to its lower amount of OOIP. It is also difficult for thicker reservoirs to achieve a miscible flooding process by injecting supercritical water steam due to the heat loss in the vertical direction. A higher cumulative SOR is detected at an early stage of SCWF for thinner reservoirs owing to their smaller OOIP. The overall performance of SCWF in a long production period is better than traditional steam flooding even without considering the impact of the aquathermolysis reaction.

3.2. Geological property – porosity

Porosity is another sensitive parameter according to the simulation as shown in Fig. 7, and it shares similar features to thickness. Lower porosity will result in a smaller OOIP in a reservoir. The cumulative oil production is not significantly impacted due to the fluctuation of porosity of the reservoir model. Therefore, a better recovery factor is being expected for lower porosity reservoirs. The simulation results also illustrate that more gas can be produced in high porosity reservoirs owing to the aquathermolysis (scenario 3) which can result in a large cumulative oil production with the same production time window. The cumulative SOR suggests that more steam is being consumed at an early stage by applying SCWF method due to the miscibility.

3.3. Geological property – permeability

The cumulative oil production and cumulative SOR are being influenced by a variation in permeability. As shown in Fig. 8, A higher permeability results in higher cumulative bitumen production for all scenarios. A lower permeability required a long time for steam to breakthrough. Thus, during the three-year production period, steam flooding (i.e., scenario 1) accounts for a better performance than SCWF without considering aquathermolysis (i.e., scenario 2) with the permeability of 200 mD due to the longer time for steam to breakthrough in SCWF. The cumulative SOR plots also demonstrate that a lower permeability reservoir generally required a long time for steam to breakthrough. Unlike porosity and thickness, a variation in permeability will not result in a change in OOIP, and thus a large recovery factor in high permeability reservoirs was being recorded in our examination.

3.4. Geological property – initial pressure

The initial reservoir pressure is not a significant influential factor on the reservoir performance for both steam flooding and SCWF (Fig. 9). The impact of the initial reservoir pressure on OOIP is also negligible in all cases. Thus, an impact of the recovery factor during the simulation time window is also negligible. However, with considering the in-situ upgrading by applying supercritical water, it was proven that larger amount bitumen was able to be extracted underground.

3.5. Operational parameters

Besides the geological properties, this paper also studied three operational parameters in the SCWF process, including an injection rate, injection steam temperature, and injector bottomhole pressure. Since the mechanism of SCWF is miscible flooding, which differs from traditional steam flooding, we only performed a sensitivity analysis for scenarios 2 and 3. Figs. 10–12 presented the cumulative bitumen produced from the reservoir and the cumulation SOR in the production time window. As a result, variations in the injection bottomhole pressure and steam temperature have no significant impact on reservoir performance as long as the miscible pressure is reached at the bottomhole condition. The maximum injection rate can positively affect the cumulative oil production, but the overall effect is negligible if considering the aquathermolysis reaction.

3.6. Recovery factor

We utilize tornado diagrams to address the impact of each sensitive parameter on the recovery factor in each scenario (Fig. 13). As a result, the recovery factors are 6.81%, 8.21% and 12.84% for the basic scenarios of steam flooding, SCWF without aquathermolysis, and SCWF with considering aquathermolysis in the three-year simulation time window. Thermal recovery techniques play a major role in all three scenarios. However, only considering the incremental heavy oil recovery due to a high temperature could lead to an underestimation effect by adopting SCWF. The impact of a chemical process between water and bitumen needs to be considered as the key mechanism during the EOR process. The SCWF can recover more bitumen even with only considering the thermal recovery mechanism in a long production time window. The in-situ upgrading consideration of aquathermolysis accounts for a significant increment of cumulative bitumen recovery (i.e., scenario 3 almost doubled the recovery factor of scenario 1 and recovered 4.63% more bitumen compared to scenario 2).

Compared to the operational parameters, the initial reservoir geologies have more impact on EOR evaluation. The results from all three scenarios demonstrate that thinner, low porosity and high permeability reservoirs can have a better performance by applying thermal recovery processes. Thickness accounts for a major consideration followed by porosity and permeability. In-situ upgrading causes approximately 35% improvement in a thinner heavy oil reservoir (i.e., thickness is 10 m in our case). The initial reservoir pressure has no significant impact in all scenarios. The only consideration during operations is the injection rate of supercritical water, but its impact is negligible compared to geological features of a reservoir. The steam temperature and pressure have no impact on reservoir performance as long as the MMP is achieved.

4. Conclusion

In this work, the numerical simulation of bitumen recovery by utilizing supercritical water was investigated with compared to a traditional thermal recovery process (i.e., steam flooding). The in-situ upgrading mechanism was considered for SCWF in our simulation. By studying the sensitivity of geological and operational characteristics, we conclude the following key findings:

(1) SCWF is a miscible flooding process accompanied with an in-situ upgrading chemical reaction, whereas traditional steam flooding is an immiscible process. The performance of SCWF is better than steam flooding in a long term due to the miscibility of water and bitumen at the early production time.
(2) In-situ upgrading is a necessity to be considered for SCWF. Gas is produced due to the aquathermolysis chemical reaction and leads to a significant increase in the recovery factor for a reservoir in the same production period compared to steam flooding.
(3) Sensitive parameters are ranked as thickness, porosity, permeability, and an injection rate. SCWF leads to outstanding performance especially in thinner, low porosity or high permeability reservoirs. A variation in the initial reservoir pressure does not affect the reservoir performance based on the results from cumulative oil production and cumulative SOR. The steam temperature and injection pressure also did not affect the reservoir performance as long as the MMP is reached.

Declaration of Competing Interest

The authors declare that they have no known competing financial interests or personal relationships that could have appeared to influence the work reported in this paper.

Acknowledgements

This research has been made possible by contributions from the Natural Sciences and Engineering Research Council (NSERC)/Energi Simulation Industrial Research Chair in Reservoir Simulation, the Alberta Innovates (iCore) Chair in Reservoir Modeling, and the Energi Simulation/Frank and Sarsh Meyer Collaboration Centre (IRCPJ 365863 – 17).

Appendix

Table A.1 Simulation results summary

No. Trails	Model	Sentative Parameter	Value	OOIP [m3]	CumOil [m3]	Cum Gas [m3]	Cum Gas to Oil	Average CumSOR	Max CumSOR	RF
Base1	M1	—	—	1.02E+05	6948.67	—	—	1.46	4.05	6.81%
Base2	M2	—	—	1.02E+05	8379.20	—	—	12.72	27.21	8.21%
Base3	M3	—	—	1.02E+05	8475.00	906959.25	4629.66	12.32	23.65	12.84%
1	M1	Thickness	10	2.34E+04	7004.07	—	—	37.96	117.37	29.91%
2	M1	Thickness	20	6.47E+04	4433.37	—	—	4.46	10.28	6.85%
3	M1	Thickness	40	1.44E+05	9369.27	—	—	0.67	1.61	6.48%
4	M1	Thickness	50	1.85E+05	11913.15	—	—	0.44	1.14	6.43%
5	M2	Thickness	10	2.34E+04	5063.01	—	—	27.94	84.49	21.62%
6	M2	Thickness	20	6.47E+04	8576.92	—	—	18.80	50.72	13.26%
7	M2	Thickness	40	1.44E+05	10906.28	—	—	9.38	15.17	7.55%
8	M2	Thickness	50	1.85E+05	15299.29	—	—	6.92	8.33	8.26%
9	M3	Thickness	10	2.34E+04	6106.60	1373159.25	7009.42	60.70	181.49	56.01%
10	M3	Thickness	20	6.47E+04	8979.65	735216.25	3752.98	18.72	42.70	19.68%
11	M3	Thickness	40	1.44E+05	7302.26	1269042.25	6477.94	9.58	17.57	9.54%
12	M3	Thickness	50	1.85E+05	15933.15	0.00	0.00	7.04	7.87	8.60%
13	M1	Average Porosity	0.1	3.39E+04	6013.38	—	—	3.22	8.23	17.72%
14	M1	Average Porosity	0.2	6.82E+04	6681.35	—	—	2.03	5.17	9.80%
15	M1	Average Porosity	0.4	1.34E+05	7072.56	—	—	1.20	3.42	5.27%
16	M1	Average Porosity	0.5	1.71E+05	7279.76	—	—	0.75	2.48	4.26%
17	M2	Average Porosity	0.1	3.39E+04	5922.33	—	—	16.20	32.48	17.45%
18	M2	Average Porosity	0.2	6.82E+04	7109.22	—	—	14.15	30.99	10.43%
19	M2	Average Porosity	0.4	1.34E+05	8518.52	—	—	11.99	25.30	6.35%
20	M2	Average Porosity	0.5	1.71E+05	9503.21	—	—	11.56	23.19	5.56%
21	M3	Average Porosity	0.1	3.39E+04	5730.55	392278.44	2002.42	18.58	29.19	22.79%
22	M3	Average Porosity	0.2	6.82E+04	6105.57	750636.81	3831.70	16.68	26.94	14.57%
23	M3	Average Porosity	0.4	1.34E+05	8518.52	1454136.13	7422.77	14.60	23.66	11.88%
24	M3	Average Porosity	0.5	1.71E+05	5691.95	1749436.50	8930.16	14.00	21.56	8.55%
25	M1	Average Perm	200	1.02E+05	3917.48	—	—	0.73	2.06	3.84%
26	M1	Average Perm	300	1.02E+05	5546.76	—	—	1.00	3.10	5.43%
27	M1	Average Perm	500	1.02E+05	9536.73	—	—	1.64	4.61	9.34%
28	M1	Average Perm	600	1.02E+05	11086.27	—	—	1.86	4.69	10.86%
29	M2	Average Perm	200	1.02E+05	3245.66	—	—	25.03	50.45	3.18%
30	M2	Average Perm	300	1.02E+05	6518.41	—	—	15.57	34.56	6.39%
31	M2	Average Perm	500	1.02E+05	10139.97	—	—	9.77	21.42	9.93%
32	M2	Average Perm	600	1.02E+05	10772.09	—	—	8.83	19.71	10.55%
33	M3	Average Perm	200	1.02E+05	2013.65	842395.50	4300.09	28.71	54.43	6.19%
34	M3	Average Perm	300	1.02E+05	3643.88	954690.88	4873.31	19.98	33.84	8.34%
35	M3	Average Perm	500	1.02E+05	9176.52	1097413.25	5601.85	11.40	17.58	14.48%
36	M3	Average Perm	600	1.02E+05	10566.98	1132136.88	5779.10	9.97	15.56	16.01%
37	M1	Pressure	7500	1.00E+05	6519.73	—	—	3.00	5.85	6.50%
38	M1	Pressure	8000	1.01E+05	6726.20	—	—	2.12	4.91	6.65%
39	M1	Pressure	9000	1.03E+05	7358.28	—	—	1.45	4.12	7.15%
40	M1	Pressure	9500	1.03E+05	7616.85	—	—	1.92	4.81	7.37%
41	M2	Pressure	7500	1.00E+05	8223.43	—	—	14.29	29.27	8.20%
42	M2	Pressure	8000	1.01E+05	7087.76	—	—	16.68	29.61	7.01%
43	M2	Pressure	9000	1.03E+05	8442.34	—	—	12.38	26.23	8.20%
44	M2	Pressure	9500	1.03E+05	8474.47	—	—	11.71	25.68	8.20%
45	M3	Pressure	7500	1.00E+05	6006.49	854762.94	4363.22	17.49	27.37	10.34%
46	M3	Pressure	8000	1.01E+05	6260.97	939378.25	4795.14	16.43	25.80	10.93%
47	M3	Pressure	9000	1.03E+05	6727.85	1116526.75	5699.41	14.65	23.22	12.07%
48	M3	Pressure	9500	1.03E+05	6891.98	1206183.63	6157.08	13.96	22.16	12.63%
49	M2	Inj rate	60	1.02E+05	8538.29	—	—	6.82	8.44	8.37%
50	M2	Inj rate	140	1.02E+05	11790.04	—	—	9.54	13.66	11.55%
51	M3	Inj rate	60	1.02E+05	6809.60	991339.44	5060.38	7.25	9.88	11.63%
52	M3	Inj rate	140	1.02E+05	8650.47	914152.00	4666.37	11.32	17.48	13.05%
53	M2	Inj pressure	30	1.02E+05	8643.75	—	—	12.70	25.69	8.47%
54	M2	Inj pressure	35	1.02E+05	8965.47	—	—	12.14	23.44	8.78%
55	M3	Inj pressure	30	1.02E+05	8556.62	915312.06	4672.30	12.33	22.62	12.96%
56	M3	Inj pressure	35	1.02E+05	7846.41	936179.00	4778.81	12.33	21.52	12.37%
57	M2	Inj Temperature	385	1.02E+05	8779.92	—	—	12.41	25.02	8.60%
58	M2	Inj Temperature	480	1.02E+05	8074.19	—	—	12.46	28.86	7.91%
59	M3	Inj Temperature	385	1.02E+05	8411.41	920615.31	4699.37	12.51	22.29	12.84%
60	M3	Inj Temperature	480	1.02E+05	8358.40	901418.81	4601.38	12.38	25.07	12.70%

References

[1] IEA, "Global Energy Review 2021," Paris, 2021. [Online]. Available: https://www.iea.org/reports/global-energy-review-2021.

[2] E. I. Administration, "International Energy Outlook 2021," 2021.

[3] Alboudwarej H, Felix J, Taylor S, Badry R, Bremner C, B. B. B, "Highlighting Heavy Oil " vol. 2, 2006.

[4] IEA, "World Energy Outlook 2020," IEA, Paris, 2020. [Online]. Available: https://www.iea.org/reports/world-energy-outlook-2020.

[5] Dusseault M, "Comparing Venezuelan and Canadian Heavy Oil and Tar Sands," In *Canadian International Petroleum Conference* Calgary, AB, Canada, 2001: Petroleum Society.

[6] Meyer RF, Attanasi ED, Freeman PA, "Heavy oil and natural bitumen resources in geological basins of the world," in "Open-File Report," U. S. Geological Survey, Report 2007-1084, 2007. [Online]. Available: http://pubs.er.usgs.gov/publication/ofr20071084.

[7] Yang S, Nie Z, Wu S, Li Z, Wang B, Wu W, et al. A critical review of reservoir simulation applications in key thermal recovery processes: lessons, opportunities,

and challenges. Energy Fuels 2021;35(9):7387–405. https://doi.org/10.1021/acs.energyfuels.1c00249.
[8] Dong X, Liu H, Chen Z, Wu K, Lu N, Zhang Q. Enhanced oil recovery techniques for heavy oil and oilsands reservoirs after steam injection. Appl Energy 2019;239:1190–211. https://doi.org/10.1016/j.apenergy.2019.01.244.
[9] Khan J, Parag D, "Twenty-Five Years of Oil Recovery by Steam Injection," In *SPE/DOE Enhanced Oil Recovery Symposium*, 1992, vol. All Days, SPE-24198-MS, doi: 10.2118/24198-ms.
[10] Chu C, "State-of-the-art review of fireflood field projects," *J. Pet. Technol.; (United States)*, pp. Medium: X; Size: Pages: 19-36, 1982.
[11] Dong M, Ma S, Liu Q. Enhanced heavy oil recovery through interfacial instability: a study of chemical flooding for Brintnell heavy oil. Fuel 2009;88(6):1049–56. https://doi.org/10.1016/j.fuel.2008.11.014.
[12] Andrianov A, Farajzadeh R, Mahmoodi Nick M, Talanana M, Zitha PLJ. Immiscible foam for enhancing oil recovery: bulk and porous media experiments. Ind Eng Chem Res 2012;51(5):2214–26. https://doi.org/10.1021/ie201872v.
[13] Guo K, Li H, Yu Z. In-situ heavy and extra-heavy oil recovery: a review. Fuel 2016;185:886–902. https://doi.org/10.1016/j.fuel.2016.08.047.
[14] Rangriz Shokri A, Babadagli T. Laboratory measurements and numerical simulation of cyclic solvent stimulation with a thermally aided solvent retrieval phase in the presence of wormholes after cold heavy oil production with sand. Energy Fuels 2016;30(11):9181–92. https://doi.org/10.1021/acs.energyfuels.6b01864.
[15] Zhao Q, Guo L, Wang Y, Jin H, Chen L, Huang Z. Enhanced oil recovery and in situ upgrading of heavy oil by supercritical water injection. Energy Fuels 2020;34(1):360–7. https://doi.org/10.1021/acs.energyfuels.9b03946.
[16] Butler RM. p. Medium: X; Size: Pages. In: Thermal recovery of oil and bitumen. Old Tappan, NJ (United States): Prentice Hall Inc.; 1991. p. 527.
[17] Speight JG. Heavy oil production processes. Gulf Professional Publishing; 2013.
[18] Dong X, Liu H, Hou J, Liu G, Chen Z, "Polymer-Enhanced Foam PEF Injection Technique to Enhance the Oil Recovery for the Post Polymer-Flooding Reservoir," presented at the SPE Western Regional Meeting, Anchorage, Alaska, USA, 2016/5/23/, 2016. [Online]. doi:10.2118/180426-MS.
[19] Hyne JB, Clark PD, Clarke RA, Koo J, Greidanus JW, "Aquathermolysis of heavy oils," *Rev. Tec. INTEVEP; (Venezuela)*, pp. Medium: X; Size: Pages: 87-94, 1982.
[20] Elahi SM, Scott CE, Chen Z, Pereira-Almao P. In-situ upgrading and enhanced recovery of heavy oil from carbonate reservoirs using nano-catalysts: upgrading reactions analysis. Fuel 2019;252:262–71. https://doi.org/10.1016/j.fuel.2019.04.094.
[21] Cheng Z-M, Ding Y, Zhao L-Q, Yuan P-Q, Yuan W-K. Effects of supercritical water in vacuum residue upgrading. Energy Fuels 2009;23(6):3178–83. https://doi.org/10.1021/ef900132z.
[22] Morimoto M, Sato S, Takanohashi T. Conditions of supercritical water for good miscibility with heavy oils. J Jpn Pet Inst 2010;53(1):61–2. https://doi.org/10.1627/jpi.53.61.
[23] Morimoto M, Sugimoto Y, Sato S, Takanohashi T. Bitumen cracking in supercritical water upflow. Energy Fuels 2014;28(2):858–61. https://doi.org/10.1021/ef401977j.
[24] Zhao Q, Guo L, Huang Z, Chen L, Jin H, Wang Y. Experimental investigation on enhanced oil recovery of extra heavy oil by supercritical water flooding. Energy Fuels 2018;32(2):1685–92. https://doi.org/10.1021/acs.energyfuels.7b03839.
[25] Canıaz RO, Erkey C. Process intensification for heavy oil upgrading using supercritical water. Chem Eng Res Des 2014;92(10):1845–63. https://doi.org/10.1016/j.cherd.2014.06.007.
[26] Guo L, Jin H. Boiling coal in water: hydrogen production and power generation system with zero net CO2 emission based on coal and supercritical water gasification. Int J Hydrogen Energy 2013;38(29):12953–67. https://doi.org/10.1016/j.ijhydene.2013.04.089.
[27] Timko MT, Ghoniem AF, Green WH. Upgrading and desulfurization of heavy oils by supercritical water. J Supercrit Fluids 2015;96:114–23. https://doi.org/10.1016/j.supflu.2014.09.015.
[28] Yan T, Xu J, Wang L, Liu Y, Yang C, Fang T. A review of upgrading heavy oils with supercritical fluids. RSC Adv 2015;5(92):75129–40. https://doi.org/10.1039/c5ra08299d.
[29] Liu Y, Bai F, Zhu C-C, Yuan P-Q, Cheng Z-M, Yuan W-K. Upgrading of residual oil in sub- and supercritical water: an experimental study. Fuel Process Technol 2013;106:281–8. https://doi.org/10.1016/j.fuproc.2012.07.032.
[30] Weingärtner H, Franck EU. Supercritical water as a solvent. Angew Chem Int Ed Engl 2005;44(18):2672–92. https://doi.org/10.1002/anie.200462468.
[31] Shah A, Fishwick R, Wood J, Leeke G, Rigby S, Greaves M. A review of novel techniques for heavy oil and bitumen extraction and upgrading. Energy Environ Sci 2010;3(6):700. https://doi.org/10.1039/b918960b.
[32] Mozaffari S, Nikookar M, Ehsani MR, Sahranavard L, Roayaie E, Mohammadi AH. Numerical modeling of steam injection in heavy oil reservoirs. Fuel 2013;112:185–92. https://doi.org/10.1016/j.fuel.2013.04.084.
[33] Chen Z. Reservoir simulation mathematical techniques in oil recovery (CBMS-NSF Regional Conference Series in Applied Mathematics). Society Ind Appl Mathematics 2007.
[34] Mehrotra AK, Eastick RR, Svrcek WY, "Viscosity of Cold Lake bitumen and its fractions," (in English), 1989-12-01 1989.
[35] Mehrotra AK, Svrcek WY. Viscosity of compressed cold lake bitumen. Can J Chem Eng 1987;65(4):672–5.
[36] Selucky ML, Chu Y, Ruo TCS, Strausz OP. Chemical composition of Cold Lake bitumen. Fuel 1978;57(1):9–16.
[37] Mehrotra AK, Svrcek WY. Properties of Cold Lake bitumen saturated with pure gases and gas mixtures. Canadian J Chem Eng 1988;66(4):656–65.
[38] S. Eghbali, H. Dehghanpour, J. Dragani, and X. Zhang, "Phase Behaviour and Viscosity of Bitumen-CO2/Light Hydrocarbon Mixtures at Elevated Temperatures: A Cold Lake Case Study," presented at the SPE Canada Heavy Oil Technical Conference, 2018. [Online]. doi:10.2118/189765-MS.
[39] Muraza O, Galadima A. Aquathermolysis of heavy oil: a review and perspective on catalyst development. Fuel 2015;157:219–31. https://doi.org/10.1016/j.fuel.2015.04.065.
[40] Maity SK, Ancheyta J, Marroquín G. Catalytic aquathermolysis used for viscosity reduction of heavy crude oils: a review. Energy Fuels 2010;24(5):2809–16. https://doi.org/10.1021/ef100230k.
[41] Hosseinpour M, Ahmadi SJ, Fatemi S. Deuterium tracing study of unsaturated aliphatics hydrogenation by supercritical water in upgrading heavy oil. Part I: non-catalytic cracking. J Supercrit Fluids 2016;107:278–85. https://doi.org/10.1016/j.supflu.2015.08.004.